Cumhuriyet Sci. J., 45(2) (2024) 322-330
DOI: https://doi.org/10.17776/csj.1452166

Cumhuriyet Science Journal

| csj.cumhuriyet.edu.tr | Founded: 2002 ISSN: 2587-2680 e-ISSN: 2587-246X Publisher: Sivas Cumhuriyet University

Polyacrylamide@Tangerine Peel Composite: A Novel Adsorbent for Efficient Removal of Pb^{2+} Ions from Water

Zeynep Mine Şenol [1,a,*]

[1] *Department of Nutrition and Diet, Faculty of Health Sciences, Sivas Cumhuriyet University, 58140 Sivas, Türkiye.*
**Corresponding author*

Research Article

History
Received: 22/03/2024
Accepted: 14/06/2024

ABSTRACT

In this study, hydrogel@fruit peel composite was synthesized by using polyacrylamide (PAA), a hydrogel, and tangerine peel (TP) as biowaste. The removal performance of PAA@TP was investigated for the Pb^{2+} ions. The FT-IR and SEM-EDX structural characterizations of PAA@TP showed that PAA@TP has various functional groups. The adsorption data fit to the isotherm models was investigated and the best fit was found with the Langmuir model. This showed that the binding sites on the surface of the PAA@TP composite showed a homogeneous distribution and that Pb^{2+} ions formed a monolayer on this homogeneous. The results show that PAA@TP can alternatively be efficiently used to treat wastewater containing Pb^{2+} ions.

Keywords: Polyacrylamide, Tangerine peel, Composite, Pb2+, Adsorption.

[a] *msenol@cumhuriyet.edu.tr* *https://orcid.org/0000-0002-5250-1267*

Introduction

With the rapid advancement of industrial activities in recent years, facilities are discharging wastewater containing heavy metals into the environment. Heavy metal pollution discharged into the environment mixes with groundwater and harms the environment [1]. This pollution mixed into water is very worrying in terms of environmental safety and public health. Because heavy metal ions cannot be biodegraded. Increasing concerns about water pollution underscore the urgent demand for effective approaches to eliminating heavy metal pollutants from water supplies [2]. The removal and recovery of heavy metals, which cause environmental pollution and harm human health, are very important. One of the dangerous heavy metals that attracts a lot of attention and causes environmental pollution is lead ions [3]. Lead is a highly toxic heavy metal and poses significant risks to both human health and aquatic ecosystems. Lead can disrupt the delicate balance of aquatic ecosystems, affecting aquatic life and overall biodiversity [4]. Long-term exposure to lead ions can cause a variety of health problems, including kidney damage, developmental disorders, and cancer. For these reasons, it is vital to remove lead from wastewater, which poses a threat to the environment and public health. Various methods such as adsorption, reverse osmosis, ion exchange, membrane filtration, and chemical precipitation are used in the treatment of heavy metals from wastewater [5]. Among these methods, the adsorption method is very interesting in terms of efficiency, low cost, and ease of application. In the adsorption method, the selection of the appropriate adsorbent is of critical importance [6]. The preferred adsorbent should be low-cost, reusable, easily accessible, and should not cause secondary pollution. In addition, the adsorbent must have advantages such as being selective to the adsorbent and having a high removal rate and capacity. Adsorbents commonly used in the removal of heavy metal ions from wastewater include various fruit peels [7], minerals [8], natural and artificial polymers [9], and composite materials [10]. The use of natural material-based composite adsorbents in the removal of heavy metal pollution has become quite widespread.

Tangerine (Citrus reticulata) is a fruit belonging to the citrus family that grows in temperate climates [11]. Vitamin A, B, C, potassium, phosphorus, calcium, etc. It has an important nutritional content for health as it contains minerals, pectin, and folic acid, is used as dietary fiber, and contains many phytochemical substances [12]. During the processing of tangerine fruits, approximately half of the fruit weight is converted into juice, while the remaining 50% is converted into peel, pulp, seeds, etc. remains as waste. While most of the acid, sugar, and mineral substances found in the fruit pass into the fruit juice, most of the water-soluble and insoluble polysaccharides, carotenoids, and lipids remain in the pulp [12]. These fruit peels, which are agricultural waste, are preferred because they are an alternative to high-cost materials in the removal of heavy metals from aqueous solutions. Overall, the interest in tangerine peels as adsorbents for different metal types and dyes underscores the potential of natural and renewable materials in addressing environmental pollution and wastewater treatment challenges.

Marques [13] used tangerine peels in the removal of Ni (II) from aqueous solutions. Unugul and Nigiz [14]

prepared activated carbon adsorbent from waste tangerine peel and used it in the removal of synthetic dyes. Husein [15] used raw and chemically modified tangerine peel for the adsorption of mercury ions. Yılmaz et al. [16] investigated the removal of Acid Brown 14 dye onto tangerine-CO TETA obtained from the tangerine peel. Inagaki et al., [17] used Mexerica tangerine (Citrus nobilis) peel to remove Cu(II), Cd(II), and Pb(II) from industrial wastewater. Özdemir et al., [18] examined the adsorption of phosphate ions and Remazol Brilliant Blue-R dye from an aqueous solution using thermally activated tangerine peel waste. Although there are many studies on using tangerine peels as adsorbents, there is no existing study on their use by creating a composite with a hydrogel. This study aims to fill this gap in the literature.

In this study, the PAA@TP composite was synthesized using tangerine peels, a biowaste, and polyacrylamide, a hydrogel, and its adsorptive properties were investigated for the removal of Pb^{2+} ion from aqueous media. PAA@TP composite was characterized by the point of zero charge (pHpzc), FT-IR, and SEM-EDX analyses. The adsorbent properties of the PAA@TP for Pb^{2+} ions were evaluated in terms of pH, concentration, kinetics, and thermodynamics of adsorption.

Materials and Methods

Chemicals and Devices

Acrylamide (AA), N, N'-methylenebisacrylamide (MBS), N, N, N', N'-tetramethylenediamine (TEMED), and ammonium persulphate (APS) were obtained from Sigma (St. Loius, MO, USA). $Pb(NO)_3$, and PAR were obtained from Merk (Germany). KNO_3, HCl, HNO_3, NaOH, ethyl alcohol, and all other chemicals were of analytical purity (Sigma Aldrich).

The functional groups on the TP, PAA@TP, and Pb^{2+} adsorbed PAA@TP were determined using the FT-IR (ATR, Bruker Model: Tensor II) technique. The surface morphology of the TP, PAA@TP, and Pb^{2+} adsorbed PAA@TP, along with the identification of different elements, was analyzed by SEM-EDX (TESCAN MIRA3 XMU).

Preparation of PAA@TP Composite

Tangerine peel was first washed with pure water and separated from its impurities. It was then left to dry at room temperature. Dried tangerine peel was ground to increase the contact surface and used in composite synthesis. To synthesize the PAA@TP composite; 1 g of tangerine peel and 1 g AA monomer were weighed and mixed in 20 mL of water in a magnetic stirrer until a homogeneous appearance was achieved. Then, MBS was added to this mixture, and mixing continued. Then, 300 µL TEMED and APS were added in a fast cycle to allow the polymerization reaction to occur. The obtained PAA@TP composite was washed with pure water until it reached approximately the conductivity of pure water. The composite was dried at 40 °C, then ground and stored in a polypropylene container.

Adsorption Procedure

Pb^{2+} adsorption studies on PAA@TP were carried out in a multiple magnetic stirrer heater by applying the batch method. Pb^{2+} ions at different concentrations and pHs were treated with adsorbent at different temperatures for varying periods. The amount of Pb^{2+} ion remaining in the solution was determined by UV-vis spectrophotometer at λ = 519 nm after complexing with PAR. Removal%, Q (mg g^{-1}), and Recovery% values were calculated using the equations below.

$$Removal\% = \left[\frac{C_i - C_f}{C_i}\right] x100 \quad (1)$$

$$Q = \left[\frac{C_i - C_f}{m}\right] xV \quad (2)$$

$$Recovery\% = \frac{Q_{des}}{Q_{ads}} x100 \quad (3)$$

Results and Discussion

FT-IR Analysis

When the FT-IR spectrum of Tangerine peel is examined (Fig. 1a), the peak around 3400 cm^{-1} is attributed to the O-H stretching vibrations of free and intermolecularly bonded hydroxyl groups [19]. The peak at 1519 cm^{-1} is attributed to C=C stretching vibrations in the aromatic rings of lignin. The peak at 2930 cm-1 is the vibrations of C-H bonds in cellulose, hemicellulose, and lignin [20]. The peak at 1234 cm^{-1} is attributed to C–O stretching vibrations in hemicellulose and lignin. The peak at 1016cm^{-1} can be attributed to the stretching vibrations of the $–OCH_3$ group of lignin to the C–O and C–H groups in cellulose. The peak at 552 cm^{-1} can be attributed to the bending vibrations of aromatic compounds [21]. In the FT-IR spectrum of the PAA@TP composite (Fig. 1a), characteristic peaks of PAA are observed. The peak at 3320 cm^{-1} is attributed to the $-CONH_2$ group and the peak at 3190 cm^{-1} is attributed to asymmetric N–H stretching vibrations. The peak at 1650 cm^{-1} is attributed to the C=O stretch in the $-CONH_2$ group. The peak at 1323 cm^{-1} is attributed to C–C stretching vibration, the peaks at 500–1300 cm^{-1} are attributed to C–H bending vibrations, and the peaks at 1000–1200 cm^{-1} are attributed to C–N stretching vibrations [22]. Characteristic peaks of TP are also seen in the FT-IR spectrum of the PAA@TP. These peaks are 3321 cm^{-1}, 2918 cm^{-1}, 1653 cm^{-1}, 1409 cm^{-1}, 1021 cm^{-1}, and 533 cm^{-1}. When the FT-IR spectrum of Pb^{2+} adsorbed PAA@TP was examined (Fig. 1b), the changes in the intensities of the peak intensities were considered as evidence of Pb^{2+} ion adsorption.

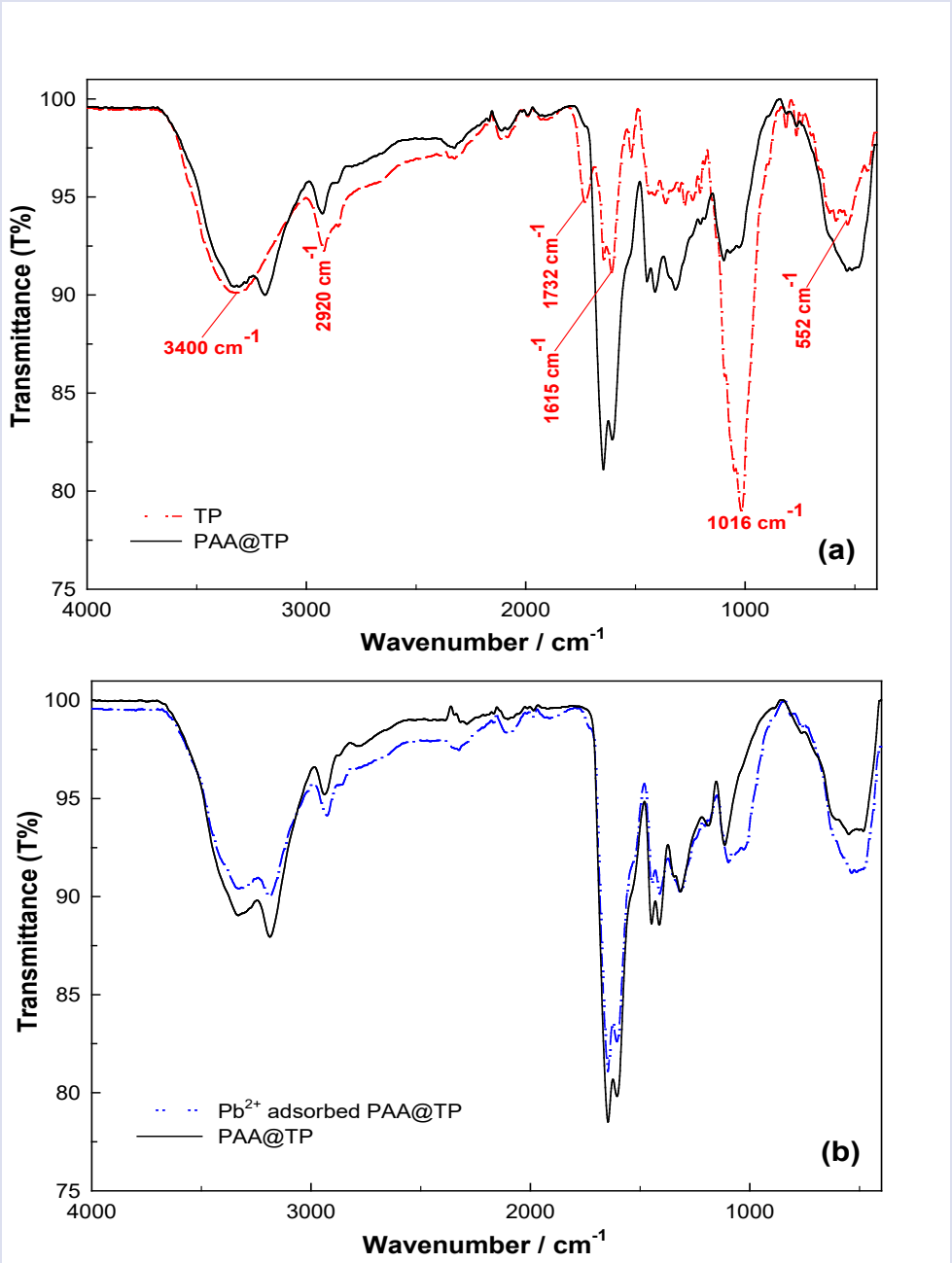

Fig. 1. FT-IR spectra of TP, PAA@TP (a) Pb^{2+} adsorbed PAA@TP (b)

SEM-EDX Analysis

The SEM morphology and EDX spectrum of pure TP (Fig. 2a-d) showed that it had an irregular and porous surface [16]. The surface morphology of the PAA@TP composite clearly shows irregular porous and rod-like structures in TP (Fig. 2b). In the SEM morphology of the Pb^{2+} adsorbed PAA@TP composite, it was seen that the pores were closed and the surface became smooth (Fig. 2c). The morphological changes observed after adsorption are thought to result from the surface complexation between the active sites and Pb^{2+} ions on the surface of the PAA@TP composite. The presence of Pb in the EDX spectrum after adsorption was evaluated as evidence of removal (Fig. 2f).

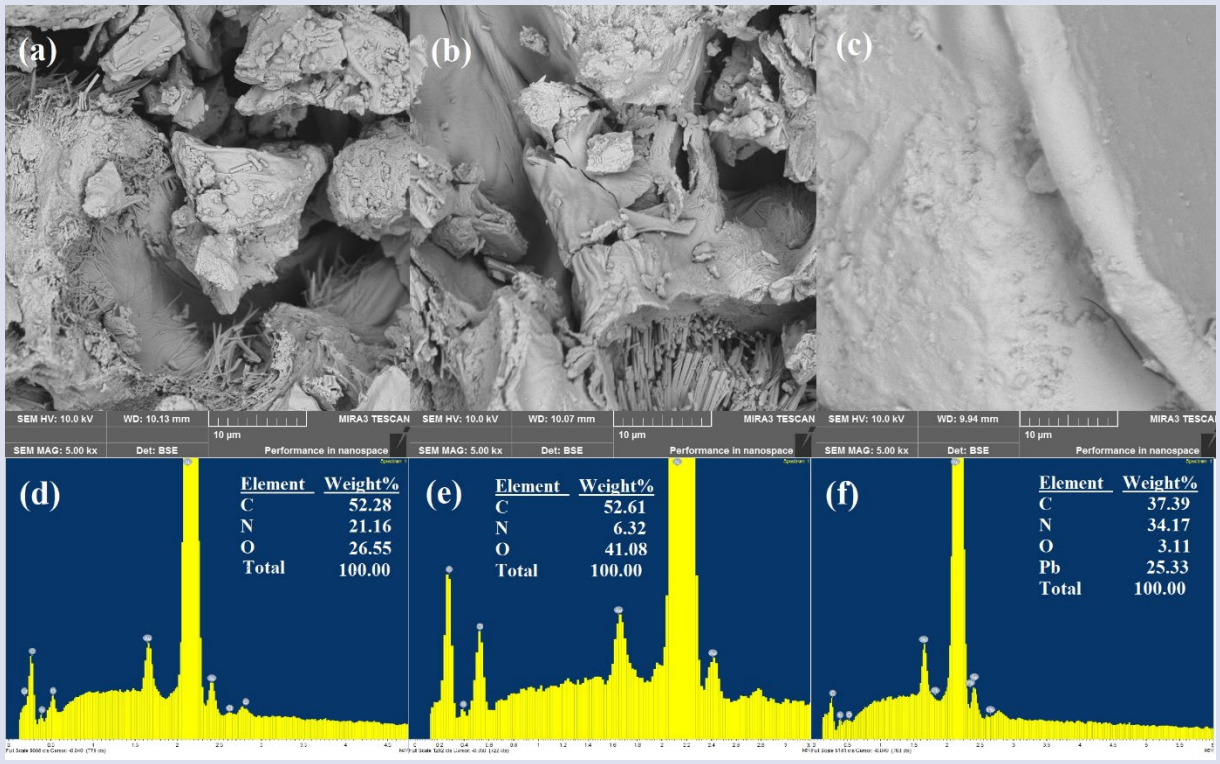

Fig. 2. SEM morphology of TP (a), PAA@TP (b), and Pb^{2+} adsorbed PAA@TP (c), and their EDX spectra, respectively (d-f)

Effect of pH

The effect of initial pH on the adsorption of Pb^{2+} ions on the PAA@TP composite was thoroughly investigated within the pH range of 1.0-5.5. The results were plotted in a pH-Q graph, depicted in Fig. 3. The graph illustrates that as the pH of the aqueous solution increases, the removal of Pb^{2+} ions also increases. At lower pH values (acidic conditions), the adsorbent surface becomes surrounded by H_3O^+ ions, resulting in positively charged surface functional groups. In such acidic conditions, H_3O^+ ions create electrostatic repulsion, hindering the approach of Pb^{2+} ions to the PAA@TP composite surface. Consequently, the efficiency of Pb^{2+} ion adsorption is low under acidic pH conditions (pH 1.0 and 2.0). As the pH of the solution increases, the competition between H_3O^+ ions and Pb^{2+} ions for binding sites on the PAA@TP surface decreases. Simultaneously, the electrostatic interaction between Pb^{2+} ions and the composite surface increases due to the decrease in positive charge density on the PAA@TP surface. This leads to enhanced adsorption efficiency. The deprotonation of active sites on the composite surface increases as the pH rises from 2.0 to 3.5, facilitating stronger electrostatic interaction between Pb^{2+} ions and the PAA@TP surface. Consequently, the adsorption capacity increases. The maximum adsorption of Pb^{2+} ions is achieved at pH 4.5. However, as the pH surpasses 5.0, the removal capacity begins to decrease. In pH regions where pH > 5.0, Pb^{2+} ions may undergo hydrolysis reactions, leading to the formation of various hydroxide species. [23]. Consequently, simultaneous adsorption and precipitation processes occur, resulting in reduced removal capacity. In summary, the pH of the solution significantly influences the adsorption of Pb^{2+} ions on the PAA@TP composite, with optimal adsorption occurring at pH 4.5. Beyond this pH, the formation of non-adsorbable hydroxide species diminishes the removal capacity.

The point of zero charge represents the pH value at which the adsorbent surface becomes electrically neutral. To determine the surface charge of the PAA@TP composite, the solid addition technique was used. In this technique, the same amount of PAA@TP composite was added to a series of solutions with the same ionic strength but different pH values. By measuring the pH values of the equilibrium solutions after waiting 24 hours, the pH at which the surface charge is neutral, that is, pHpzc, was determined. The solid addition technique allows researchers to systematically vary the pH of the solution while keeping other parameters constant. This information is crucial to understand the adsorption behavior of the composite under different pH conditions and to optimize its performance in practical applications [24]. The pHpzc value for the PAA@TP composite was determined to be 5.11, as shown in **Fig. 3.** This pH value indicates the point at which the surface of the composite becomes electrically neutral. At solution pH values lower than the pHpzc value (pHpzc>pH), the surface of the composite carries a net positive charge, while at solution pH values greater than the pHpzc value (pHpzc<pH), it carries a net negative charge on the composite This information is crucial for understanding the adsorption behavior of the PAA@TP composite, especially about pH-dependent processes such as electrostatic interactions with adsorbate species.

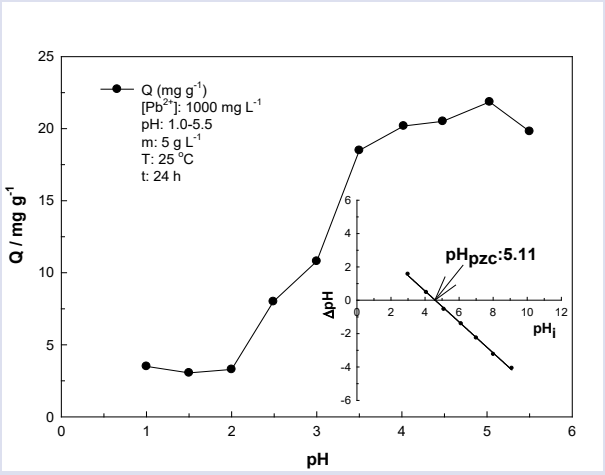

Fig. 3. Effect of pH and pHpzc

Effect of Adsorbent Dose

In experiments designed to evaluate the effect of adsorbent dose, the PAA@TP composite was used in amounts ranging from 1 to 20 g L^{-1}. The relationship between the adsorbent dose and adsorbed amount is shown in Fig. 4. It is seen that as the amount of adsorbent increases, the number of active adsorption sites also increases. Despite the increase in active centers, the concentration of Pb^{2+} ions in the solution remains constant. It was observed that increasing the adsorbent dose from 1 g L^{-1} to 20 g L^{-1} led to an increase in the removal percentage from 12% to 70%. This observation underlines the importance of optimizing the adsorbent dose in adsorption processes. By appropriately adjusting the adsorbent dose, researchers can maximize the use of active adsorption sites and increase the efficiency of removing contaminants from the solution.

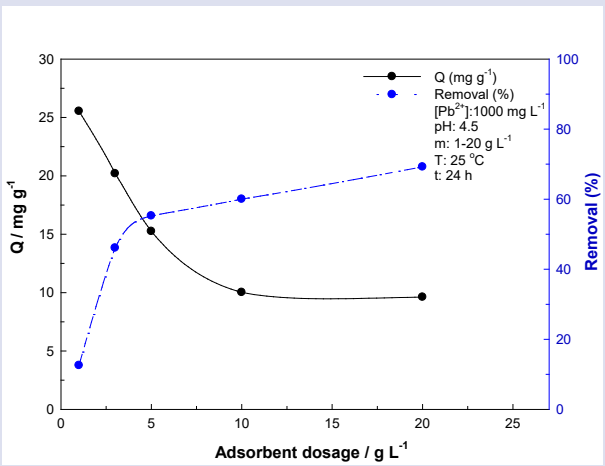

Fig. 4. Effect of adsorbent dose

Adsorption Isotherms

To examine the nature of the adsorption process of Pb^{2+} ions onto the PAA@TP composite, Langmuir, Freundlich, and Dubinin-Radushkevich (D-R) isotherm models were applied to the obtained data. The Langmuir isotherm model [25] is based on the assumption that there is a fixed number of active centers with equal energy on the homogeneous adsorbent surface. The Freundlich isotherm model [26] assumes the existence of different types of adsorptive areas on a heterogeneous surface. The D-R isotherm model [27] examines the nature of adsorption on a heterogeneous surface, especially in porous adsorbents, and evaluates the adsorption process from an energetic perspective.

The fit of the Langmuir, Freundlich, and D-R isotherm models for the adsorption of Pb^{2+} ions onto the PAA@TP composite is shown in Fig. 5, and the parameters of the isotherm models are summarized in Table 1. When the correlation coefficients of the Langmuir and Freundlich isotherm models were examined, it was seen that the correlation coefficient of the Langmuir model was greater than the correlation coefficient of the Freundlich model. This shows that the active centers on the surface of the PAA@TP composite are distributed homogeneously and Pb^{2+} ions form a single layer on this homogeneous surface. The adsorption capacity was determined as 27.3 mg g^{-1}. In addition, the β value of 0.330 obtained from the Freundlich isotherm equation shows the feasibility of adsorption. From the D-R isotherm model, the E_{DR} value calculated as 14.7 kJ mol^{-1} and E_{DR} > 8 kJ mol^{-1}, it can be inferred that the adsorption of Pb^{2+} ions on PAA@TP occurs in the form of chemical adsorption.

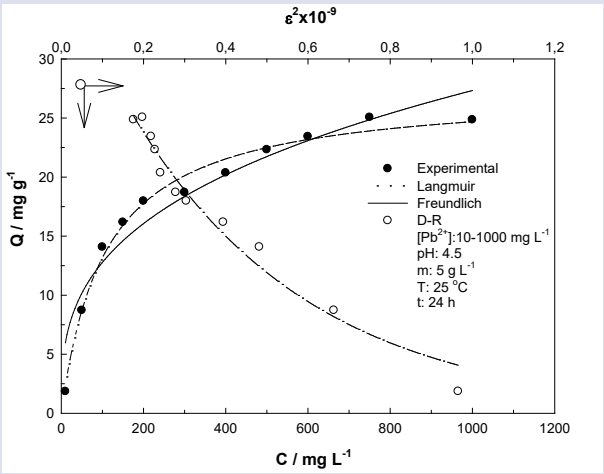

Fig. 5. Adsorption isotherms

Table 1. The parameters of isotherm models

Isotherm Model	Parameter	Value
Langmuir $Q = \frac{Q_L C_e}{1 + K_L C_e}$	Q_L (mg g^{-1})	27.3
	K_L (L mg^{-1})	0.00927
	R^2	0.988
Freundlich $Q = X_F C_e^{\beta}$	X_F	2.79
	β	0.330
	R^2	0.935
D-R $Q = X_{DR} e^{-(K_{DR}\varepsilon^2)}$ $\varepsilon = RT\ln\left(1 + \frac{1}{C_e}\right)$ $E_{DR} = (2K_{DR})^{-0.5}$	X_{DR} (mg g^{-1})	37.8
	$-K_{DR}x10^9$/mol^2 KJ^{-2}	2.13
	E_{DR}/kJ mol^{-1}	14.7
	R^2	0.973

A comparison of the Pb^{2+} ion adsorption capacity of the PAA@TP composite with other adsorbents reported in the literature is presented in Table 2. Examining Table 2, it was seen that the efficiency of Pb^{2+} ion removal by the PAA@TP composite was higher than that of many other adsorbents. This comparison highlights the superior performance of the PAA@TP composite in removing Pb^{2+} ions from aqueous solutions, highlighting its potential as an effective adsorbent for wastewater treatment and environmental remediation applications.

Table 2. The comparison of Pb^{2+} ion adsorption capacities of various adsorbents found in the literature

Adsorbent	pH	Q/ mg g^{-1} from Langmuir model	Reference
MoS_2-clinoptilolite	6.0	3.45	[28]
Waste beer yeast	1.0-5.0	2.34	[29]
Peels of banana	5.0	2.18	[30]
Waste beer yeast	1.0-5.0	2.34	[29]
Coconut	4.0	4.38	[31]
Okra waste	5.0	5.0	[32]
Pinus Nigra Tree Bark	8.0	12.6	[33]
Chitosan-GLA beads	4.5	14.24	[34]
Coir	4.9	0.127	[35]
Hydroxyapatite–chitosan composite	7.0	12.04	[36]
PAA@TP	4.5	27.3	This study

Adsorption Kinetics

Adsorption kinetics is very important as it provides valuable information about the adsorption mechanism and helps optimize adsorption processes for the effective removal of heavy metal pollutants from wastewater. The effect of interaction time on the adsorption of Pb^{2+} ions by PAA@TP was investigated at time intervals ranging from 10 to 1440 min, as shown in Fig. 6. Looking at Fig. 6, the adsorption occurs quickly due to the presence of empty adsorptive sites on the PAA@TP composite surface. As the equilibrium time is approached, the adsorption rate gradually slows down. This phenomenon indicates that Pb^{2+} ions gradually penetrated the pores of the PAA@TP composite. Further examination of Fig. 6 showed that the time required for Pb^{2+} adsorption to reach equilibrium was approximately 180 min. A significant increase in adsorption was observed beyond this stage, indicating that the adsorption centers had become saturated.

The kinetic models used for describing the adsorption process are represented by the equations given in Table 3. The corresponding graphs of the pseudo-1st-order (PFO) [37], pseudo-2nd-order (PSO) [38], and intra-particle diffusion (IPD) [39] models are depicted in Fig. 6, and the calculated results from these models are summarized in Table 3. Standard regression coefficient (R^2) values were compared to evaluate the applicability of the PFO and PSO models. It was seen that the R^2 value for the PSO model (R^2: 0.907) was greater than the value of the PFO model (R^2: 0.881). It also showed that the PSO model provided a better fit to the experimental data, with the calculated Q_t agreeing more closely with the experimental Q_e values. Additionally, the fit of the experimental data to the IPD model graph was examined to determine the mechanism involved in the adsorption process. The multicollinearity observed in the IPD plot presented in Fig. 6 indicates that two or more steps are involved in the adsorption process. The bilge linearity observed in the IPD plot indicates the presence of both film and pore diffusion mechanisms. Overall, the kinetic results showed that the adsorption process of Pb^{2+} ions onto the PAA@TP composite followed multiple steps characterized by IPD and PSO patterns.

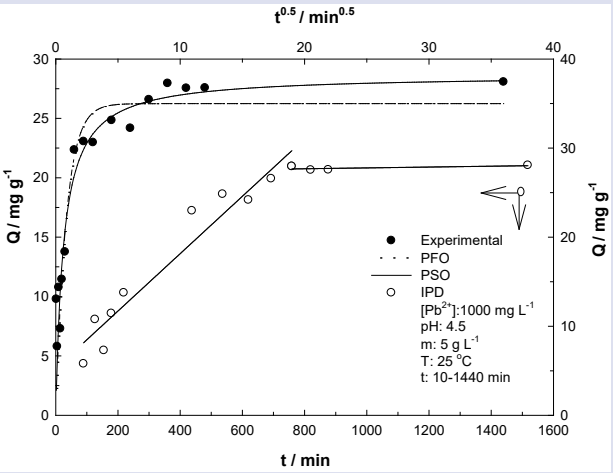

Fig. 6. Adsorption kinetics

Table 3. The parameters of kinetic models

Kinetic model	Parameter	Value
PFO	Q_t / mg g^{-1}	28.1
$Q_t = Q_e[1 - e^{-k_1 t}]$	Q_e / mg g^{-1}	26.2
$H_1 = k_1 Q_e$	k_1 x10^3/min^{-1}	29.3
	H_1x10^3/mg$g^{-1}min^{-1}$	770
	R^2	0.881
PSO	Q_t/ mg g^{-1}	28.1
$Q_t = \frac{t}{\left[\frac{1}{k_2 Q_e^2}\right] + \left[\frac{t}{Q_e}\right]}$	Q_e / mg g^{-1}	28.7
	k_2x10^3/$mg^{-1}gmin^{-1}$	1.39
	H_2x10^3/mg g^{-1} min^{-1}	1145
$H_2 = k_2 Q_e^2$	R^2	0.907
IPD	k_i x10^3/mg g^{-1} $min^{-0.5}$	5261
$Q_t = k_i t^{0.5}$	R^2	0.936

Adsorption Thermodynamics

The effect of temperature on the adsorption process is a critical aspect to consider in adsorption studies. Thermodynamic parameters such as ΔG°, ΔH°, and ΔS° were calculated using the following equations [40].

$$K_d = \frac{Q}{C_e} \quad (4)$$

$$lnK_D = \frac{\Delta S^\circ}{R} - \frac{\Delta H^\circ}{RT} \quad (5)$$

$$\Delta G^o = \Delta H^o - T\Delta S^o \quad (6)$$

The Van't Hoff graph was plotted to observe the effect of temperature on adsorption (Fig. 7), and the resulting thermodynamic parameters are summarized in Table 4. The standard enthalpy value was found to be -22.7 kJ mol^{-1}. The fact that the adsorption process was exothermic showed that increasing the temperature led to a decrease in the adsorption capacity. The entropy value was found to be -47.8 J mol^{-1} K^{-1}. In addition, negative values of ΔG° indicated that the nature of the adsorption was thermodynamically feasible and spontaneous. Overall, these findings showed that the adsorption process was affected by temperature and followed an exothermic path.

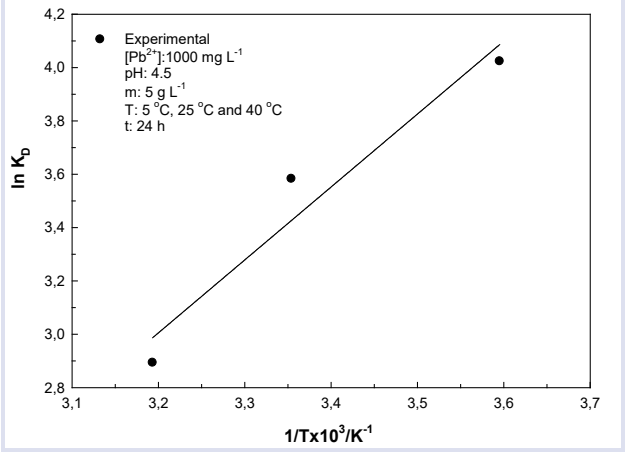

Fig. 7. Adsorption thermodynamics

Tablo 4. Thermodynamic parameters

Temperature/°C	ΔH°/kJ mol^{-1}	ΔG°/kJ mol^{-1}	ΔS°/J mol^{-1} K^{-1}	R²
5		-9.40		
25	-22.7	-8.45	-47.8	0.936
40		-7.73		

Reusability

In adsorption studies, the reusability and recovery of the adsorbent are crucial factors to consider. Therefore, it is essential to investigate the desorption behavior of the PAA@TP composite used for removing Pb^{2+} ions. To examine the desorption of Pb^{2+} ions from the PAA@TP composite, three solvents were utilized: 1 mol L^{-1} solutions of HCl, NaOH, and ethyl alcohol. After subjecting the composite to three desorption cycles, it was observed that HCl achieved the highest yield of desorption, with a rate of 57% (as shown in **Fig. 8**). This finding demonstrated that HCl was the most effective solvent for removing Pb^{2+} ions from the PAA@TP composite, leading to a relatively high recovered ion yield.

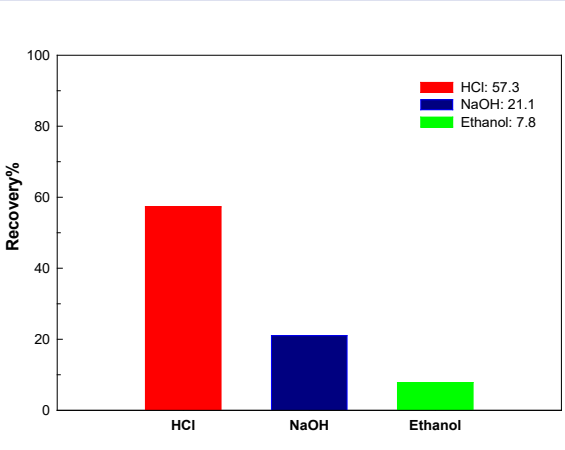

Fig. 8. The effect of desorption on PAA@TP

Conclusion

In this article, the adsorption of Pb^{2+} ions on the PAA@TP composite used as an adsorbent was thoroughly investigated. Various experimental parameters such as pH, contact time, adsorbent dose, initial concentration of the solution, and temperature were systematically varied to optimize the adsorption conditions. Optimum removal conditions were determined as pH 4.5, adsorbent dose 5 g L^{-1}, 24-hour contact time, and 25°C temperature. Experimental data were applied to Langmuir, Freundlich, and D-R isotherms models. Among these models, the Langmuir model showing monolayer adsorption behavior showed the best fit to the experimental data. Under optimum conditions, the monolayer adsorption capacity was determined as 27.3 mg g^{-1}. Adsorption kinetics showed that the adsorption process followed the PSO and IPD models. Adsorption thermodynamics showed that the adsorption process was exothermic and spontaneous. All these findings showed that the PAA@TP composite is a useful, cost-effective, and promising adsorbent for the removal of Pb^{2+} ions from wastewater.

Acknowledgments

The present study was partially supported by the Sivas Cumhuriyet University Projects Commission.

Conflict of interest

The authors declare that they have no competing interests

References

[1] Razzak S.A., Faruque M.O., Alsheikh Z., Alsheikhmohamad L., Alkuroud D., Alfayez A., Hossain S.M.Z., Hossain M.M., A comprehensive review on conventional and biological-driven heavy metals removal from industrial wastewater, *Environ. Adv*., 7 (2022) 100168.

[2] Qu X., Brame J., Li Q., Alvarez P.J.J., Nanotechnology for a safe and sustainable water supply: Enabling integrated water treatment and reuse, *Acc. Chem. Res*., 46(3) (2013) 834-843.

[3] Arbabi M., Hemati S., Amiri M., Removal of lead ions from industrial wastewater: A review of Removal methods, *Int. J. Epidemiol. Res*., 4 (2015) 10.

[4] Jayasri M.A., Suthindhiran K., Effect of zinc and lead on the physiological and biochemical properties of aquatic plant Lemna minor: its potential role in phytoremediation, *Appl. Water Sci*., 7 (2017).

[5] Chaemiso, T. D., Nefo, T. Removal methods of heavy metals from laboratory wastewater, *J. Nat. Sci. Res*., 9(2) (2019) 36-42.

[6] Iftekhar S., Ramasamy D. L., Srivastava V., Asif M. B., Sillanpää M., Understanding the factors affecting the adsorption of Lanthanum using different adsorbents: a critical review. *Chemosphere*., 204 (2018) 413-430.

[7] Feng, N., Guo, X., Liang, S. Adsorption study of copper (II) by chemically modified orange peel, *J. Hazard. Mater*., 164 (2009) 1286-1292.

[8] ElSayed, E. E. . Natural diatomite as an effective adsorbent for heavy metals in water and wastewater treatment (a batch study), *Water Sci.,* 32(1) (2018) 32-43.

[9] Arslan, D. Ş., Ertap, H., Şenol, Z. M., El Messaoudi, N., Mehmeti, V. Preparation of polyacrylamide titanium dioxide hybrid nanocomposite by direct polymerization and its applicability in removing crystal violet from aqueous solution, *J. Polym. Environ*., (2023) 1-15.

[10] Şen, N. E., Şenol, Z. M. Effective removal of Allura red food dye from water using cross-linked chitosan-diatomite composite beads, *Int. J. Biol. Macromol*., 253 (2023) 126632.

[11] Denkova-Kostova, R., Teneva, D., Tomova, T., Goranov, B., Denkova, Z., Shopska, V., Hristova-Ivanova, Y. Chemical composition, antioxidant and antimicrobial activity of essential oils from tangerine (Citrus reticulata L.), grapefruit (Citrus paradisi L.), lemon (Citrus lemon L.) and cinnamon (Cinnamomum zeylanicum Blume), *Sect. C. J. Biosci.,* 76(5-6), (2021) 175-185.

[12] Bureš, M. S., Maslov Bandić, L., Vlahoviček-Kahlina, K. Determination of bioactive components in mandarin fruits: A review, *Crit. Rev. Anal. Chem*., 53(7) (2023) 1489-1514.

[13] da Costa Marques, V. Valorization of Tangerine Peels in the Preparation of Adsorbents for Removal of Ni (II) From Aqueous Solutions (Master's thesis, Instituto Politecnico de Braganca (Portugal), (2020).

[14] Unugul T., Nigiz F. U. Preparation and characterization of an active carbon adsorbent from waste mandarin peel and determination of adsorption behavior on removal of synthetic dye solution, *Air. Soil Pollut.,* 231(11) (2020) 538.

[15] Husein D. Z. Adsorption and removal of mercury ions from aqueous solution using raw and chemically modified Egyptian mandarin peel, *Desalin. Water Treat*., 51(34-36) (2013). 6761-6769.

[16] Yılmaz M., Eldeeb, T. M., Hassaan, M. A., El-Nemr, M. A., Ragab, S., El Nemr, A. The use of mandarin-biochar-O3-TETA (MBT) produced from mandarin peels as a natural adsorbent for the removal of acid red 35 (AR35) dye from water, *Environ. Process*., 9(3) (2022) 44.

[17] Inagaki C. S., Caretta T. D. O., Alfaya R. V. D. S., Alfaya A. A. D. S. Mexerica mandarin (Citrus nobilis) peel as a new biosorbent to remove Cu (II), Cd (II), and Pb (II) from industrial effluent, Desalin, *Water Treat*., 51(28-30) (2013) 5537-5546.

[18] Özdemir N. C., Bilici, Z., Saleh M., Dizge N. Adsorption of phosphate ions and RBBR dye from aqueous solution using thermally activated mandarin peel waste, *Water Pract. Technol*., 19(1) (2024) 170-180.

[19] Torab M. M., Biosorption of lanthanum and cerium from aqueous solutions using tangerine (Citrus reticulata) peel: equilibrium, kinetic and thermodynamic studies, *Chem. Ind. Chem. Eng. Q*., 19(1) (2013) 79-88.

[20] Pavan F. A., Mazzocato A. C., Jacques R. A., Dias, S. L. Ponkan peel: a potential biosorbent for removal of Pb (II) ions from aqueous solution, *Biochem. Eng. J*., 40(2) (2008) 357-362.

[21] Abdić Š., Memić M., Šabanović E., Sulejmanović J., Begić S. Adsorptive removal of eight heavy metals from aqueous solution by unmodified and modified agricultural waste: tangerine peel, *Int. J. Environ. Sci. Technol*. 15 (2018) 2511-2518.

[22] Chiem L. T., Huynh L., Ralston J., Beattie, D. A., An in situ ATR–FTIR study of polyacrylamide adsorption at the talc surface, *J. Colloid Interface Sci*. 297(1), (2006) 54-61.

[23] Yurishcheva A.A., Sorption of Pb^{2+} by magnetite coated with humic acids, *J. Biol. Phys. Chem*. 13 (2013) 61-68.

[24] Şenol Z.M., Gül Ü.D., Gürkan R., Bio-sorption of bisphenol a by the dried- and inactivated-lichen (Pseudoevernia furfuracea) biomass from aqueous solutions, *J. Environ. Heal. Sci. Eng.,* 18 (2020) 853-864.

[25] Langmuir I., The adsorption of gases on plane surfaces of glass, mica and platinum, *J. Am. Chem. Soc.,* 40(9) (1918) 1361-1403.

[26] Freundlich H., Über die Adsorption in Lösungen, *Zeitschrift Für Phys. Chemie.* 57(1) (1907) 385-470.

[27] Hu, Q., & Zhang, Z. (2019). Application of Dubinin–Radushkevich isotherm model at the solid/solution interface: A theoretical analysis, *J. Mol. Liq.,* 277 (2019) 646-648.

[28] Pandey S., Fosso-Kankeu E., Spiro M. J., Waanders, F., Kumar, N., Ray, S. S., Kang, M. Equilibrium, kinetic, and thermodynamic studies of lead ion adsorption from mine wastewater onto MoS2-clinoptilolite composite, *Mater. Today Chem.,* 18 (2020) 100376.

[29] Parvathi K., Nagendran R., Nareshkumar R., Lead biosorption onto waste beer yeast by-product: a means to decontaminate effluent generated from the battery manufacturing industry, *Electron. J. Biotechnol.* 10(1) (2007) 92-105.

[30] Anwar, J., Shafique, U., Salman, M., Dar, A., & Anwar, S. (2010). Removal of Pb (II) and Cd (II) from water by adsorption on peels of banana, *Bioresour. Technol*., 101(6) (2010) 1752-1755.

[31] Gueu, S., Yao, B., Adouby, K., Ado, G. Kinetics and thermodynamics study of lead adsorption on to activated carbons from coconut and seed hull of the palm tree, Int. *J. Environ. Sci. Technol.* 4 (2007) 11-17.

[32] Hashem M. A. (2007). Adsorption of lead ions from aqueous solution by okra wastes, *Int. J. Phys. Sci.,* 2(7) (2007) 178-184.

[33] Argun M. E., Dursun S. Activation of pine bark surface with NaOH for lead removal, *J. Int. Environ. Appl. Sci*., 2 (2007) 5-10.

[34] Ngah, W. W., Fatinathan, S. Pb (II) biosorption using chitosan and chitosan derivatives beads: Equilibrium, ion exchange and mechanism studies, *J. Environ. Sci.,* 22(3) (2010) 338-346.

[35] Shukla S. R., Pai R. S. Removal of Pb (II) from solution using cellulose-containing materials, *J. Chem. Technol. Biotechnol*., 80(2) (2005) 176-183.

[36] Gupta N., Kushwaha A. K., Chattopadhyaya, M. C. Adsorptive removal of Pb2+, Co2+ and Ni2+ by hydroxyapatite/chitosan composite from aqueous solution, *J. Taiwan Inst. Chem. Eng*. 43(1), (2012) 125-131.

[37] Ho, Y. S., McKay, G. Kinetic models for the sorption of dye

from aqueous solution by wood, *Process Saf. Environ. Prot*., 76(2) (1998) 183-191.

[38] Ho, Y. S., McKay, G. Pseudo-second order model for sorption processes, *Process Biochem*., 34(5) (1999) 451-465.

[39] Weber Jr, W. J., Morris, J. C. Kinetics of adsorption on carbon from solution, *J. Sanit. Eng. Div.,* 89(2) (1963) 31-59.

[40] Hong, S., Wen, C., He, J., Gan, F., Ho, Y. S. Adsorption thermodynamics of methylene blue onto bentonite, *J. Hazard. Mater*., 167(1-3) (2009) 630-633.